LUND UNIVERSITY

Cramér-Rao bounds for determination of permittivity and permeability in slabs

Sjöberg, Daniel; Larsson, Christer

2010

Link to publication

Citation for published version (APA):
Sjöberg, D., & Larsson, C. (2010). *Cramér-Rao bounds for determination of permittivity and permeability in slabs*. (Technical Report LUTEDX/(TEAT-7190)/1-13/(2010)). Electromagnetic Theory Department of Electrical and Information Technology Lund University Sweden.

Total number of authors:
2

General rights
Unless other specific re-use rights are stated the following general rights apply:
Copyright and moral rights for the publications made accessible in the public portal are retained by the authors and/or other copyright owners and it is a condition of accessing publications that users recognise and abide by the legal requirements associated with these rights.
• Users may download and print one copy of any publication from the public portal for the purpose of private study or research.
• You may not further distribute the material or use it for any profit-making activity or commercial gain
• You may freely distribute the URL identifying the publication in the public portal

Read more about Creative commons licenses: https://creativecommons.org/licenses/

Take down policy
If you believe that this document breaches copyright please contact us providing details, and we will remove access to the work immediately and investigate your claim.

LUND UNIVERSITY

PO Box 117
221 00 Lund
+46 46-222 00 00

Download date: 18. Dec. 2025

CODEN:LUTEDX/(TEAT-7190)/1-13/(2010)

Cramér-Rao bounds for determination of permittivity and permeability in slabs

Daniel Sjöberg and Christer Larsson

Electromagnetic Theory
Department of Electrical and Information Technology
Lund University
Sweden

Daniel Sjöberg
Daniel.Sjoberg@eit.lth.se

Department of Electrical and Information Technology
Electromagnetic Theory
Lund University
P.O. Box 118
SE-221 00 Lund
Sweden

Christer Larsson
Christer.Larsson@saabgroup.com
Christer.Larsson@eit.lth.se

Saab Bofors Dynamics AB
SE-581 88 Linköping
Sweden

Department of Electrical and Information Technology
Electromagnetic Theory
Lund University
P.O. Box 118
SE-221 00 Lund
Sweden

Editor: Gerhard Kristensson
© Daniel Sjöberg and Christer Larsson, Lund, March 30, 2010

Abstract

We compute the Cramér-Rao lower bounds for determination of isotropic permittivity and permeability in slabs using scattering data such as reflection and transmission coefficients. Assuming only the fundamental mode is propagating in the slab, the results are formally the same regardless if the slab is in free space, or inside a rectangular or coaxial waveguide. The bounds depend only on signal quality and not the actual inversion method used, making them suitable to evaluate a particular measurement setup. The results are illustrated with several measurements in a rectangular waveguide setting.

1 Introduction

When measuring the electromagnetic properties of materials, it is common to manufacture a sample in the form of a planar slab and measure the reflection and transmission through the slab [2, 6]. Three common measurement setups are in a hollow rectangular waveguide, in a coaxial cable, or as a free space measurement. As long as only one mode can be expected in the waveguide or coaxial cable, all three setups have very similar mathematical models. In the waveguide, there is always some dispersion due to the confined geometry, which corresponds to the free space case where the angle of incidence is varying with frequency in such a way that the transverse wave number is constant [8, 19].

In order to estimate the permittivity and permeability from reflection and transmission measurements, the Nicolson-Ross-Weir method is commonly used [18, 22]. This is an explicit inversion of the scattering parameters to obtain the material parameters ϵ and μ, the only point of ambiguity being to determine how many wavelengths that can fit inside the slab. This ambiguity can often be resolved by unwrapping the phase information in the transmission data starting from low frequencies, where the number of wavelengths inside the slab can be assumed less than one if the slab is thin enough. Another classical shortcoming of the NRW method is that it breaks down when the slab is lossless and half a wavelength in thickness. Several methods have been proposed to deal with this problem [1, 3, 5]. In this paper we clarify that the problem does not depend on the inversion algorithm as such, but is due to poor signal quality in reflection data, since there is perfect transmission through a half wavelength slab. If the inversion is based on transmission data only, no problem occurs.

Alternative inversion methods are often based on optimization approaches, setting up a material model with suitable degrees of freedom and computing synthetic scattering parameters. These scattering parameters are then compared with the measured ones, and the material parameters are tuned to minimize the difference [1]. This procedure has the advantage that it is possible to enforce material models with a physically reasonable frequency dependence satisfying the Kramers-Kronig relations [10, 15, 17].

Although different inversion procedures have been around for a long time, there is still limited understanding of their inherent limitations, such as what errors can be

expected in different parameter regions when noise is present. This question has a precise answer in the case when all systematic errors have been eliminated. We can then study the Fisher information matrix, the inverse of which gives us the variance of the parameters we wish to estimate [16]. This provides a theoretical framework for the error analysis in [3], which can be generalized to other measurement situations, for instance involving more complex material parameters [7, 9, 13, 14, 20].

2 The Fisher information matrix

Assume we can measure complex reflection and transmission coefficients r and t for an isotropic slab with thickness d at a certain frequency. The electromagnetic material parameters for the slab are the relative complex permittivity ϵ and the relative complex permeability μ, and we wish to estimate them from r and t. The Fisher information matrix is [16, 21]

$$\mathcal{I} = \frac{1}{\sigma_r^2}\begin{pmatrix}\frac{\partial r}{\partial \epsilon}\\ \frac{\partial r}{\partial \mu}\end{pmatrix}\begin{pmatrix}\frac{\partial r}{\partial \epsilon} & \frac{\partial r}{\partial \mu}\end{pmatrix}^* + \frac{1}{\sigma_t^2}\begin{pmatrix}\frac{\partial t}{\partial \epsilon}\\ \frac{\partial t}{\partial \mu}\end{pmatrix}\begin{pmatrix}\frac{\partial t}{\partial \epsilon} & \frac{\partial t}{\partial \mu}\end{pmatrix}^* \tag{2.1}$$

$$= \frac{1}{\sigma_r^2}\begin{pmatrix}\left|\frac{\partial r}{\partial \epsilon}\right|^2 & \frac{\partial r}{\partial \epsilon}\left(\frac{\partial r}{\partial \mu}\right)^*\\ \frac{\partial r}{\partial \mu}\left(\frac{\partial r}{\partial \epsilon}\right)^* & \left|\frac{\partial r}{\partial \mu}\right|^2\end{pmatrix} + \frac{1}{\sigma_t^2}\begin{pmatrix}\left|\frac{\partial t}{\partial \epsilon}\right|^2 & \frac{\partial t}{\partial \epsilon}\left(\frac{\partial t}{\partial \mu}\right)^*\\ \frac{\partial t}{\partial \mu}\left(\frac{\partial t}{\partial \epsilon}\right)^* & \left|\frac{\partial t}{\partial \mu}\right|^2\end{pmatrix} \tag{2.2}$$

where σ_r is the noise level for the reflection coefficient, and σ_t is the noise level for the transmission coefficient. Note that the matrix is hermitian symmetric by construction. The Cramér-Rao lower bound is [12, 16]

$$\mathrm{var}(\epsilon) \geq [\mathcal{I}^{-1}]_{\epsilon\epsilon} \tag{2.3}$$

$$\mathrm{var}(\mu) \geq [\mathcal{I}^{-1}]_{\mu\mu} \tag{2.4}$$

which can be used to compute the limit of the accuracy for the parameters estimated from the measurement. When plotting the bounds in Figures 2 and 3, we plot the bound for the standard deviation (the square root of the variance), *i.e.*, $([\mathcal{I}^{-1}]_{\epsilon\epsilon})^{1/2}$ and $([\mathcal{I}^{-1}]_{\mu\mu})^{1/2}$ in dB scale.

To compute the Fisher information matrix, we need an explicit expression for the reflection and transmission coefficients. These are given by [4]

$$r = \frac{r_0(1-\mathrm{e}^{-2\mathrm{j}\beta d})}{1-r_0^2\mathrm{e}^{-2\mathrm{j}\beta d}} \tag{2.5}$$

$$t = \frac{(1-r_0^2)\mathrm{e}^{-\mathrm{j}\beta d}}{1-r_0^2\mathrm{e}^{-2\mathrm{j}\beta d}} \tag{2.6}$$

for a slab surrounded by free space. If the slab is backed by metal, the reflection coefficient is

$$r_{\mathrm{PEC}} = \frac{r_0-\mathrm{e}^{-2\mathrm{j}\beta d}}{1-r_0\mathrm{e}^{-2\mathrm{j}\beta d}} \tag{2.7}$$

The reflection and transmission coefficients depend in their turn on the interface reflection coefficient $r_0 = (Z-Z_0)/(Z+Z_0)$ and the wave number in the material

β, where Z and Z_0 are the wave impedances in the slab and in the surrounding free space, respectively. The detailed dependence of the wave parameters Z and β on the material parameters ϵ and μ depend on polarization and measurement setup, and can be found in Appendix A, where also the explicit formulas for the relevant derivatives can be found.

Instead of calculating the information matrix with respect to the material parameters ϵ and μ, we could compute it with respect to the wave parameters β and Z, or more preferably their normalized values $\bar{\beta} = \beta/k_0$ and $\bar{Z} = Z/\eta_0$, where $k_0 = \omega\sqrt{\epsilon_0\mu_0}$ is the wave number in free space and $\eta_0 = \sqrt{\mu_0/\epsilon_0}$ is the wave impedance in free space. The Fisher information matrix is then

$$\mathcal{I}_{\text{wave}} = \frac{1}{\sigma_r^2}\begin{pmatrix} \left|\frac{\partial r}{\partial \bar{\beta}}\right|^2 & \frac{\partial r}{\partial \bar{\beta}}\left(\frac{\partial r}{\partial \bar{Z}}\right)^* \\ \frac{\partial r}{\partial \bar{Z}}\left(\frac{\partial r}{\partial \bar{\beta}}\right)^* & \left|\frac{\partial r}{\partial \bar{Z}}\right|^2 \end{pmatrix} + \frac{1}{\sigma_t^2}\begin{pmatrix} \left|\frac{\partial t}{\partial \bar{\beta}}\right|^2 & \frac{\partial t}{\partial \bar{\beta}}\left(\frac{\partial t}{\partial \bar{Z}}\right)^* \\ \frac{\partial t}{\partial \bar{Z}}\left(\frac{\partial t}{\partial \bar{\beta}}\right)^* & \left|\frac{\partial t}{\partial \bar{Z}}\right|^2 \end{pmatrix} \tag{2.8}$$

where the derivatives are computed from the derivatives in Appendix A as

$$\frac{\partial r}{\partial \bar{\beta}} = k_0\frac{\partial r}{\partial \beta} \qquad \frac{\partial r}{\partial \bar{Z}} = \eta_0\frac{\partial r}{\partial r_0}\frac{\partial r_0}{\partial Z} \tag{2.9}$$

$$\frac{\partial t}{\partial \bar{\beta}} = k_0\frac{\partial t}{\partial \beta} \qquad \frac{\partial t}{\partial \bar{Z}} = \eta_0\frac{\partial t}{\partial r_0}\frac{\partial r_0}{\partial Z} \tag{2.10}$$

This allows us to calculate the Cramér-Rao lower bounds for the variance of the normalized wave parameters $\bar{\beta}$ and $\bar{Z}$ as

$$\text{var}(\bar{\beta}) \geq [\mathcal{I}_{\text{wave}}^{-1}]_{\bar{\beta}\bar{\beta}} \tag{2.11}$$

$$\text{var}(\bar{Z}) \geq [\mathcal{I}_{\text{wave}}^{-1}]_{\bar{Z}\bar{Z}} \tag{2.12}$$

When plotting these bounds in Figures 2 and 3, we plot the bounds corresponding to the standard deviations, *i.e.*, $([\mathcal{I}^{-1}]_{\bar{\beta}\bar{\beta}})^{1/2}$ and $([\mathcal{I}^{-1}]_{\bar{Z}\bar{Z}})^{1/2}$ in dB scale. In the inversion algorithm, $\bar{\beta}$ basically involves the product $\epsilon\mu$ and $\bar{Z}$ involves primarily the ratio μ/ϵ, although the case is complicated at oblique incidence as can be seen from the explicit expressions for β and Z in Appendix A.

3 Computer program

The Cramér-Rao lower bounds have been implemented with a GUI in python,[1] see Figure 1. The code is available by contacting the authors. Using this program, the influence of a number of parameters can be studied. Three measurement setups are implemented:

- Rectangular waveguide (with arbitrary width)
- Coaxial cable

[1] http://www.python.org

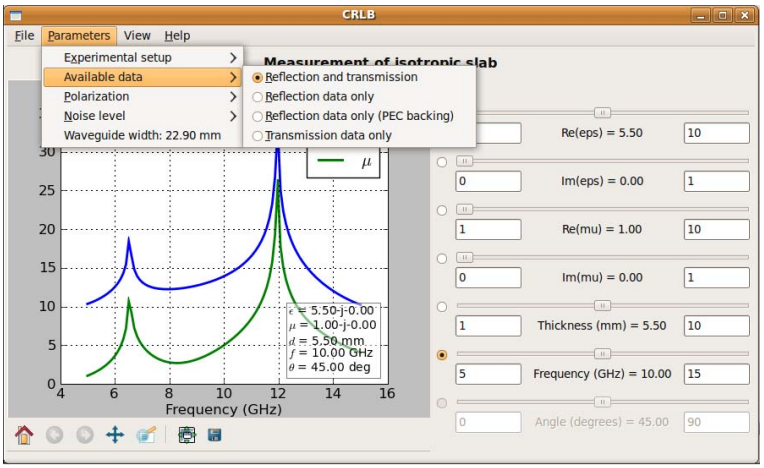

Figure 1: Screen shot of python implementation of the Cramér-Rao lower bound. Using the menus and the sliders, many different combinations of parameters can be investigated. The resulting figures can be saved in a variety of vector or bitmap formats.

- Free space plane wave (with arbitrary angle of incidence and TE or TM polarization)

The coaxial cable case is mathematically identical to the free space plane wave for normal incidence, but is included for convenience since it is a common measurement setup. Furthermore, the noise levels in reflection and transmission can be set separately. The Cramér-Rao lower bounds can be plotted for either ϵ and μ or β/k_0 and Z/η_0, against any of the parameters $\mathrm{Re}(\epsilon)$, $\mathrm{Im}(\epsilon)$, $\mathrm{Re}(\mu)$, $\mathrm{Im}(\mu)$, thickness d, frequency f, or (in the plane wave case) angle of incidence θ.

Using this program, graphs such as those shown in Figure 2 can be generated. The curves should be interpreted such that the standard deviation of the estimation of each parameter can not be less than the values given by the corresponding curve, at a given noise level. The bounds are plotted at unit noise level ($\sigma_r = \sigma_t = 0\,\mathrm{dB}$), and changing the noise level only shifts the curves up or down by the corresponding amount. For instance, the bound for ϵ at 10 GHz is at about 14 dB in Figure 2. This means that in order to get an estimation of ϵ with two digits of accuracy (relative error of at most 0.05 or $-13\,\mathrm{dB}$), the noise level must be kept below $-27\,\mathrm{dB}$.

In Figure 2 it is seen that the Cramér-Rao lower bounds for the material parameters ϵ and μ increase at two frequencies: the cutoff frequency for the waveguide, and the resonance frequency where the length of the slab corresponds to one half wavelength in the material. It is also seen that only the bound for the normalized wave impedance $\bar{Z} = Z/\eta_0$ increases at the resonance frequency. Thus, the inherent difficulty in determining both ϵ and μ at this frequency is due only to the difficulty in determining *one* of the wave parameters β and Z. In other words, this means that knowledge of one parameter (for instance $\mu = 1$ for non-magnetic materials), means the other parameter can be determined in a stable way.

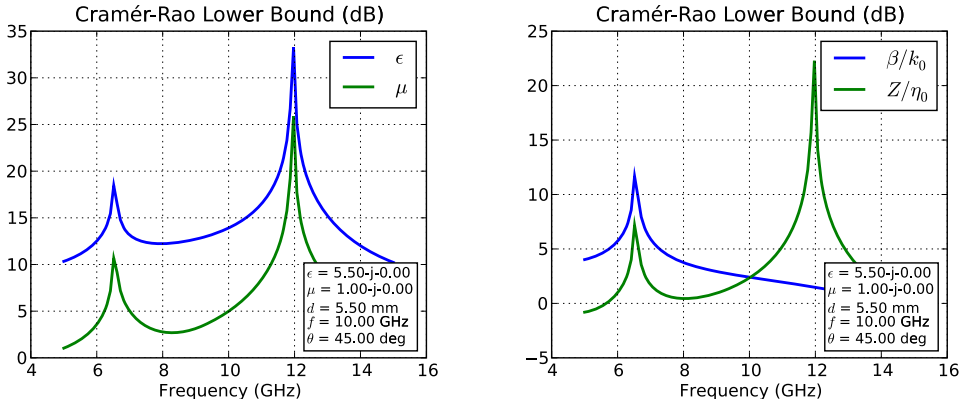

Figure 2: Cramér-Rao lower bounds for material parameters (left) and wave parameters (right), for a lossless dielectric slab in a rectangular waveguide. It is seen that the bounds for both ϵ and μ are increased at cutoff frequency (6.55 GHz) and resonance frequency (half wavelength slab, 12 GHz). However, it is seen that only the bound for the wave impedance is increased at the resonance frequency.

At the resonance frequency, the reflection is low (ideally zero), making it difficult to estimate the wave impedance $\bar{Z}$. This is an artefact of lossless slabs; by introducing losses, the peak in the Cramér-Rao lower bound for $\bar{Z}$ is significantly lowered, see Figure 3.

4 Measurements

To verify the theoretical predictions of the Cramér-Rao lower bounds, the following experimental test has been performed. The S-parameters for several dielectric slabs were measured in an X-band (8–12 GHz) waveguide fixture using a Performance Network Analyzer (PNA). The measurements were repeated for different source power levels in order to vary the signal to noise ratio. A TRL calibration [11] was performed for each source power level before the measurement. Samples of epoxy and Macor® were used in the measurements. Macor has a dielectric constant of 5.67 and a loss tangent of $7.1 \cdot 10^{-3}$ at 8.5 GHz.[2] The resulting data was evaluated with the Nicolson-Ross-Weir method [18, 22] to calculate the material parameters ϵ and μ, as well as the wave parameters $\bar{\beta}$ and $\bar{Z}$. The measurement system is shown in Figure 4.

The results for a reference epoxy slab, known to have virtually constant material parameters in the X-band, are shown in Figure 5. It is seen that all parameters of interest are very smooth functions of frequency. There is no resonance, since the slab is shorter than half a wavelength in the entire frequency band.

In Figure 6 the results for a thick slab of Macor is shown. Here, a clear resonance occurs at about 8.5 GHz, corresponding to a thickness of half a wavelength in the

[2] http://www.corning.com/docs/specialtymaterials/pisheets/Macor.pdf

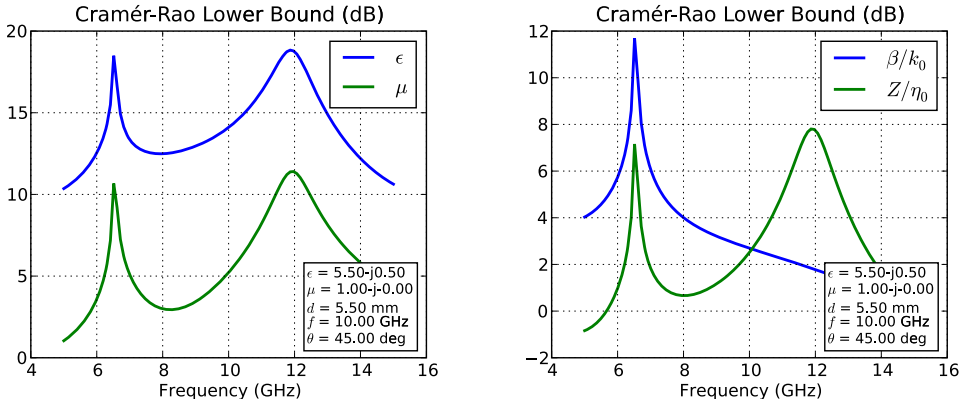

Figure 3: Cramér-Rao lower bounds for the same case as in Figure 2, except that some dielectric losses have been added. The peaks at the resonance are significantly lower than in Figure 2.

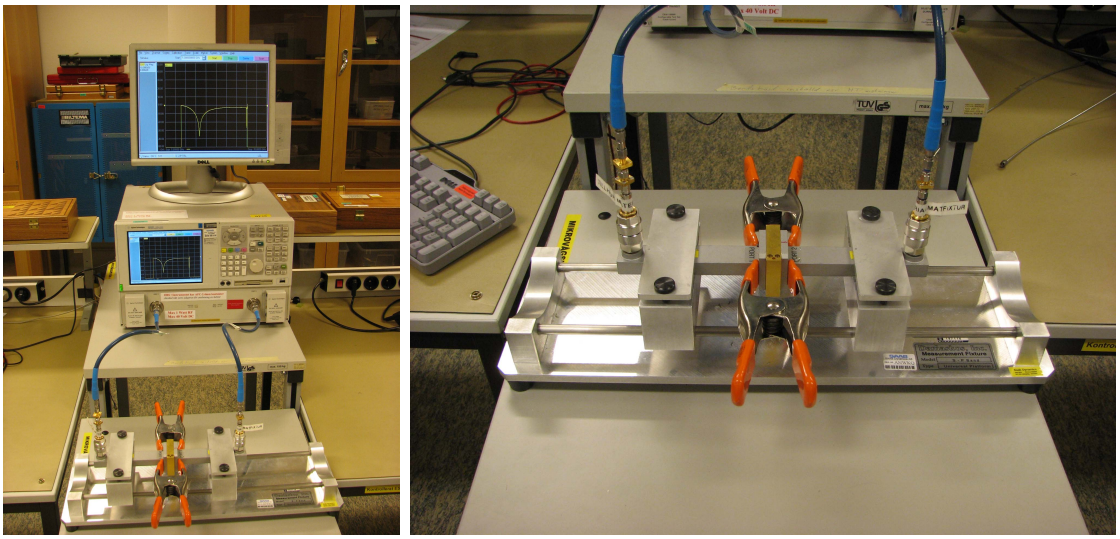

Figure 4: The measurement system. A network analyzer is connected to two waveguide segments, joined by a sample holder containing the material under test.

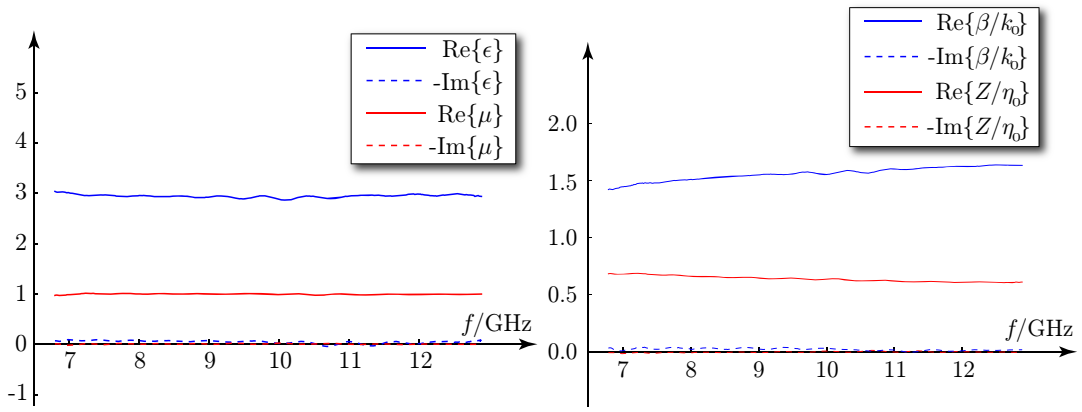

Figure 5: The measured material and wave parameters for a slab of epoxy with length 5.1 mm, which is short enough not to cause any resonances in the frequency interval considered. To the left is the determination of the material parameters ϵ and μ, and to the right is the determination of the wave parameters β/k_0 and Z/η_0. Measurement data is only available in the interval where one single mode is propagating in the empty waveguide.

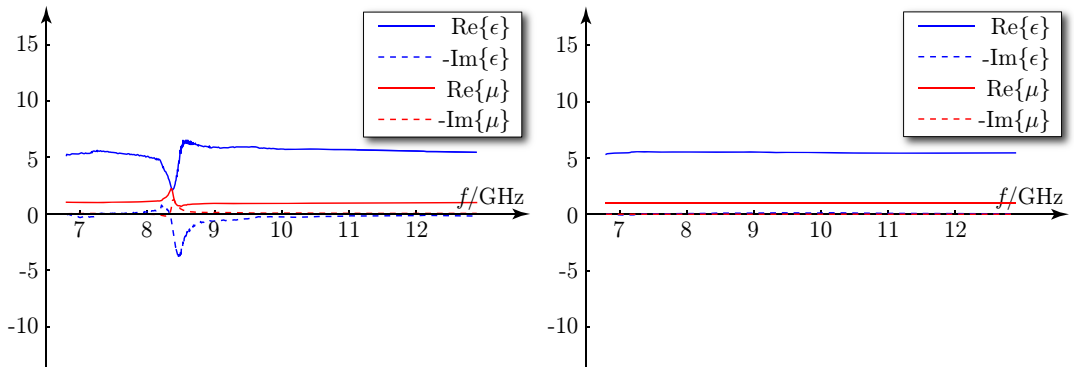

Figure 6: The measured material parameters for a thick slab of Macor (ℓ = 8.0 mm), where a resonance occurs at about 8.5 GHz. To the left is the full determination of both ϵ and μ, and to the right it is assumed that the material is non-magnetic, $\mu = 1$.

material. It is clearly seen that both the material parameters permittivity and permeability are difficult to determine accurately in the vicinity of this frequency. The algorithm even generates an imaginary part of ϵ with the wrong sign (passive materials must have constant sign in the imaginary part of ϵ and μ). When considering the wave parameters, only the relative impedance $\bar{Z} = Z/\eta_0$ is resonant, whereas the relative wavenumber $\bar{\beta} = \beta/k_0$ behaves smoothly throughout the interval, see Figure 7. The difficulties in determining ϵ disappear if we assume that the material is non-magnetic ($\mu = 1$), and compute ϵ from the wave number β only. The result is the graph to the right in Figure 6.

We finally consider the influence of noise. In Figure 7, the measured material and wave parameters are shown for varying signal-to-noise levels. It is seen that the noise causes most problems in the region around the resonance, and the wave number β/k_0 remains relatively well determined even though the simultaneous computation of ϵ and μ produces bad results. Thus, the permittivity ϵ can be determined with precision for non-magnetic materials, even with noisy data, by enforcing *a priori* knowledge of the permeability $\mu = 1$.

5 Conclusions

The Cramér-Rao lower bound describes how well we can estimate a certain parameter from measurement data. We have calculated the explicit bounds for determining permittivity and permeability from reflection and transmission data for slabs. Furthermore, we have shown that the frequency variation of the bounds agrees with basic physical phenomena, such as the cutoff frequency phenomenon in waveguides, and the half wavelength resonance in slabs. Using these bounds, it is possible to estimate the minimum signal to noise ratio needed to estimate the material parameters with a given accuracy.

A drawback of the Cramér-Rao lower bounds, is that they only apply to a situation where all the systematic errors have been eliminated and (Gaussian zero-mean) noise is the only remaining source of error. The systematic error is difficult to suppress in real situations, and the eventual success of the measurement is very much linked to the calibration procedure.

A particular result of this paper is that the half wavelength resonance in slabs influences only the impedance and not the estimation of the wave number in the slab. We can not extract any information on wave impedance for this frequency unless a slab with different thickness is used, or if we combine information from neighboring frequency points with a hypothesis that the material properties do not change very much. However, this leads to an arbitrariness which is undesirable in real measurement systems.

6 Acknowledgements

This work is a result of an exchange programme between Lund University and Saab Bofors Dynamics AB, sponsored by the Swedish Foundation for Strategic Research. The support of all these organizations is gratefully acknowledged.

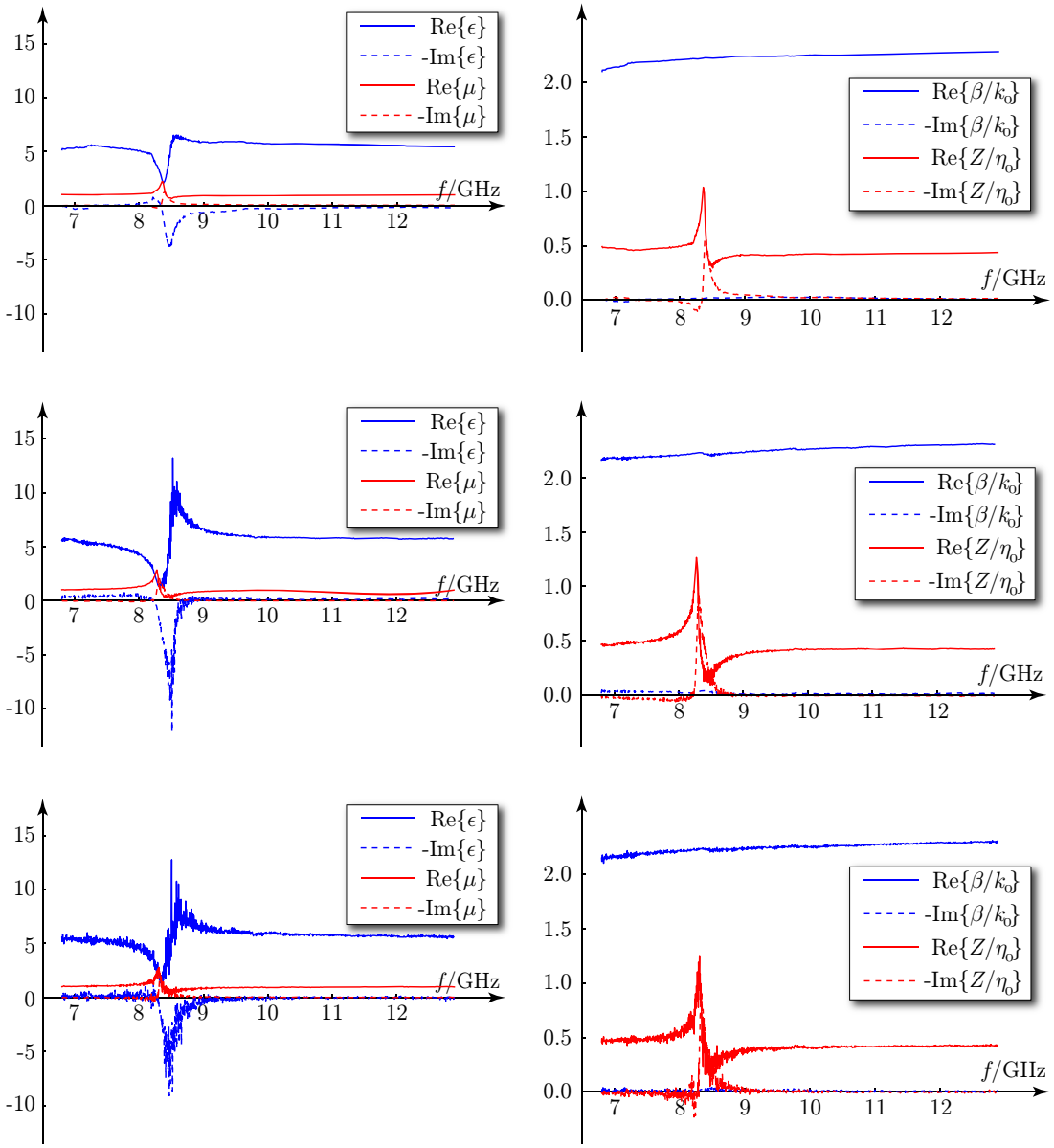

Figure 7: The measured material and wave parameters for thick slabs of Macor with varying noise levels. The noise level was controlled by setting the source power level in the network analyzer to 0 dBm (top graphs), −20 dBm (middle graphs), and −40 dBm (bottom graphs). Thus, the noise level differ by 20 dB between each set of graphs.

Appendix A Calculation of some derivatives

In this Appendix we calculate the explicit expressions for the derivatives that make up the Fisher information matrix in (2.2) and (2.8). The reflection and transmission coefficients for a slab surrounded by free space are [4]

$$r = \frac{r_0(1-\mathrm{e}^{-2\mathrm{j}\beta d})}{1-r_0^2\mathrm{e}^{-2\mathrm{j}\beta d}} \tag{A.1}$$

$$t = \frac{(1-r_0^2)\mathrm{e}^{-\mathrm{j}\beta d}}{1-r_0^2\mathrm{e}^{-2\mathrm{j}\beta d}} \tag{A.2}$$

If the slab is backed by metal, the reflection coefficient is

$$r_{\mathrm{PEC}} = \frac{r_0-\mathrm{e}^{-2\mathrm{j}\beta d}}{1-r_0\mathrm{e}^{-2\mathrm{j}\beta d}} \tag{A.3}$$

The parameters involved are

$$r_0 = \frac{Z-Z_0}{Z+Z_0} \tag{A.4}$$

$$Z = \begin{cases} \frac{\eta k}{\beta} = \eta_0\frac{k_0\mu}{\beta} & \mathrm{TE} \\ \frac{\eta\beta}{k} = \eta_0\frac{\beta}{k_0\epsilon} & \mathrm{TM} \end{cases} \tag{A.5}$$

$$Z_0 = \begin{cases} \frac{\eta_0 k_0}{\beta_0} & \mathrm{TE} \\ \frac{\eta_0\beta_0}{k_0} & \mathrm{TM} \end{cases} \tag{A.6}$$

where ϵ_0 and μ_0 are the permittivity and permeability of free space, ϵ and μ are the relative permittivity and permeability of the material, $k_0 = \omega\sqrt{\epsilon_0\mu_0}$ and $k = k_0\sqrt{\epsilon\mu}$ are the wave numbers in free space and in the material, $\eta_0 = \sqrt{\mu_0/\epsilon_0}$ and $\eta = \eta_0\sqrt{\mu/\epsilon}$ are the wave impedances in free space and in the material, $\beta_0 = \sqrt{k_0^2-k_{\mathrm{t}}^2}$ and $\beta = \sqrt{k^2-k_{\mathrm{t}}^2}$ are the longitudinal wavenumbers in free space and in the material, and k_{t} is the transverse wavenumber. For the TE_{10} mode in a rectangular waveguide, we have $k_{\mathrm{t}} = \pi/a$, where a is the width of the waveguide, and for a plane wave normally incident on a slab we have $k_{\mathrm{t}} = k_0\sin\theta$, where θ is the angle of incidence.

Using the chain rule, we now have

$$\frac{\partial r}{\partial\epsilon} = \frac{\partial r}{\partial r_0}\frac{\partial r_0}{\partial Z}\frac{\partial Z}{\partial\epsilon} + \frac{\partial r}{\partial\beta}\frac{\partial\beta}{\partial\epsilon} \tag{A.7}$$

which shows that all derivatives can be computed from a few canonical derivatives. These are as follows.

$$\frac{\partial r}{\partial r_0} = \frac{\partial}{\partial r_0}\frac{r_0(1-\mathrm{e}^{-2\mathrm{j}\beta d})}{1-r_0^2\mathrm{e}^{-2\mathrm{j}\beta d}} = \frac{1-\mathrm{e}^{-2\mathrm{j}\beta d}}{1-r_0^2\mathrm{e}^{-2\mathrm{j}\beta d}} + \frac{2r_0^2\mathrm{e}^{-2\mathrm{j}\beta d}(1-\mathrm{e}^{-2\mathrm{j}\beta d})}{(1-r_0^2\mathrm{e}^{-2\mathrm{j}\beta d})^2} \tag{A.8}$$

$$\frac{\partial r}{\partial\beta} = \frac{\partial}{\partial\beta}\frac{r_0(1-\mathrm{e}^{-2\mathrm{j}\beta d})}{1-r_0^2\mathrm{e}^{-2\mathrm{j}\beta d}} = 2\mathrm{j}d\left(\frac{r_0\mathrm{e}^{-2\mathrm{j}\beta d}}{1-r_0^2\mathrm{e}^{-2\mathrm{j}\beta d}} - \frac{r_0(1-\mathrm{e}^{-2\mathrm{j}\beta d})r_0^2\mathrm{e}^{-2\mathrm{j}\beta d}}{(1-r_0^2\mathrm{e}^{-2\mathrm{j}\beta d})^2}\right) \tag{A.9}$$

$$\frac{\partial t}{\partial r_0} = \frac{\partial}{\partial r_0}\frac{(1-r_0^2)\mathrm{e}^{-\mathrm{j}\beta d}}{1-r_0^2\mathrm{e}^{-2\mathrm{j}\beta d}} = \frac{-2r_0\mathrm{e}^{-\mathrm{j}\beta d}}{1-r_0^2\mathrm{e}^{-2\mathrm{j}\beta d}} + \frac{2r_0\mathrm{e}^{-2\mathrm{j}\beta d}(1-r_0^2)\mathrm{e}^{-\mathrm{j}\beta d}}{(1-r_0^2\mathrm{e}^{-2\mathrm{j}\beta d})^2} \tag{A.10}$$

$$\frac{\partial t}{\partial \beta} = \frac{\partial}{\partial \beta}\frac{(1-r_0^2)\mathrm{e}^{-\mathrm{j}\beta d}}{1-r_0^2\mathrm{e}^{-2\mathrm{j}\beta d}} = \mathrm{j}d\left(\frac{-(1-r_0^2)\mathrm{e}^{-\mathrm{j}\beta d}}{1-r_0^2\mathrm{e}^{-2\mathrm{j}\beta d}} - \frac{(1-r_0^2)\mathrm{e}^{-\mathrm{j}\beta d}r_0^2 2\mathrm{e}^{-2\mathrm{j}\beta d}}{(1-r_0^2\mathrm{e}^{-2\mathrm{j}\beta d})^2}\right) \tag{A.11}$$

$$\frac{\partial r_0}{\partial Z} = \frac{\partial}{\partial Z}\frac{Z-Z_0}{Z+Z_0} = \frac{1}{Z+Z_0} - \frac{Z-Z_0}{(Z+Z_0)^2} = \frac{2Z_0}{(Z+Z_0)^2} \tag{A.12}$$

$$\frac{\partial Z_{\mathrm{TE}}}{\partial \epsilon} = \eta_0\frac{\partial}{\partial \epsilon}\frac{k_0\mu}{\beta} = -\eta_0\frac{k_0\mu}{\beta^2}\frac{\partial \beta}{\partial \epsilon} = -\frac{Z}{\beta}\frac{\partial \beta}{\partial \epsilon} \tag{A.13}$$

$$\frac{\partial Z_{\mathrm{TM}}}{\partial \epsilon} = \eta_0\frac{\partial}{\partial \epsilon}\frac{\beta}{k_0\epsilon} = \eta_0\left(-\frac{\beta}{k_0\epsilon^2} + \frac{1}{k_0\epsilon}\frac{\partial \beta}{\partial \epsilon}\right) = -\frac{Z}{\epsilon} + \frac{Z}{\beta}\frac{\partial \beta}{\partial \epsilon} \tag{A.14}$$

$$\frac{\partial Z_{\mathrm{TE}}}{\partial \mu} = \eta_0\frac{\partial}{\partial \mu}\frac{k_0\mu}{\beta} = \eta_0\left(\frac{k_0}{\beta} - \frac{k_0\mu}{\beta^2}\frac{\partial \beta}{\partial \mu}\right) = \frac{Z}{\mu} - \frac{Z}{\beta}\frac{\partial \beta}{\partial \mu} \tag{A.15}$$

$$\frac{\partial Z_{\mathrm{TM}}}{\partial \mu} = \eta_0\frac{\partial}{\partial \mu}\frac{\beta}{k_0\epsilon} = \eta_0\frac{1}{k_0\epsilon}\frac{\partial \beta}{\partial \mu} = \frac{Z}{\beta}\frac{\partial \beta}{\partial \mu} \tag{A.16}$$

$$\frac{\partial \beta}{\partial \epsilon} = \frac{\partial}{\partial \epsilon}\sqrt{k^2-k_{\mathrm{t}}^2} = \frac{1}{2}\frac{2k}{\sqrt{k^2-k_{\mathrm{t}}^2}}\frac{\partial k}{\partial \epsilon} = \frac{k}{\beta}k_0\sqrt{\mu}\frac{1}{2\sqrt{\epsilon}} = \frac{k^2}{2\beta\epsilon} \tag{A.17}$$

$$\frac{\partial \beta}{\partial \mu} = \frac{\partial}{\partial \mu}\sqrt{k^2-k_{\mathrm{t}}^2} = \frac{1}{2}\frac{2k}{\sqrt{k^2-k_{\mathrm{t}}^2}}\frac{\partial k}{\partial \mu} = \frac{k}{\beta}k_0\sqrt{\epsilon}\frac{1}{2\sqrt{\mu}} = \frac{k^2}{2\beta\mu} \tag{A.18}$$

For a metal backed slab we also need the derivatives

$$\frac{\partial r_{\mathrm{PEC}}}{\partial r_0} = \frac{\partial}{\partial r_0}\frac{r_0-\mathrm{e}^{-2\mathrm{j}\beta d}}{1-r_0\mathrm{e}^{-2\mathrm{j}\beta d}} = \frac{1}{1-r_0\mathrm{e}^{-2\mathrm{j}\beta d}} + \frac{r_0-\mathrm{e}^{-2\mathrm{j}\beta d}}{(1-r_0\mathrm{e}^{-2\mathrm{j}\beta d})^2}\mathrm{e}^{-2\mathrm{j}\beta d} \tag{A.19}$$

$$\frac{\partial r_{\mathrm{PEC}}}{\partial \beta} = \frac{\partial}{\partial \beta}\frac{r_0-\mathrm{e}^{-2\mathrm{j}\beta d}}{1-r_0\mathrm{e}^{-2\mathrm{j}\beta d}} = 2\mathrm{j}d\left(\frac{\mathrm{e}^{-2\mathrm{j}\beta d}}{1-r_0\mathrm{e}^{-2\mathrm{j}\beta d}} - \frac{r_0-\mathrm{e}^{-2\mathrm{j}\beta d}}{(1-r_0\mathrm{e}^{-2\mathrm{j}\beta d})^2}r_0\mathrm{e}^{-2\mathrm{j}\beta d}\right) \tag{A.20}$$

References

[1] J. Baker-Jarvis, R. G. Geyer, and P. D. Domich. A nonlinear least-squares solution with causality constraints applied to transmission line permittivity and permeability determination. *IEEE Trans. Instrumentation and Measurement*, **41**(5), 646–652, 1992.

[2] J. Baker-Jarvis, R. G. Geyer, J. John H. Grosvenor, M. D. Janezic, C. A. Jones, B. Riddle, and C. M. Weil. Dielectric characterization of low-loss materials: A comparison of techniques. *IEEE Transactions on Dielectrics and Electrical Insulation*, **5**(4), 571–577, August 1998.

[3] J. Baker-Jarvis, E. J. Vanzura, and W. A. Kissick. Improved technique for determining complex permittivity with the transmission/reflection method. *IEEE Trans. Microwave Theory Tech.*, **38**(8), 1096–1103, August 1990.

[4] M. Born and E. Wolf. *Principles of Optics*. Cambridge University Press, Cambridge, U.K., seventh edition, 1999.

[5] A.-H. Boughriet, C. Legrand, and A. Chapoton. Noniterative stable transmission/reflection method for low-loss material complex permittivity determination. *IEEE Trans. Microwave Theory Tech.*, **45**, 52–57, 1997.

[6] L. F. Chen, C. K. Ong, C. P. Neo, V. V. Varadan, and V. K. Varadan. *Microwave electronics: Measurement and materials characterisation*. John Wiley & Sons, New York, 2004.

[7] X. Chen, T. M. Gzegorczyk, and J. A. Kong. Optimization approach to the retrieval of he constitutive parameters of a slab of general bianisotropic medium. *Progress in Electromagnetics Research*, **60**, 1–18, 2006.

[8] R. E. Collin. *Field Theory of Guided Waves*. IEEE Press, New York, second edition, 1991.

[9] N. J. Damaskos, R. B. Mack, A. L. Maffett, W. Parmon, and P. L. E. Uslenghi. The inverse problem for biaxial materials. *IEEE Trans. Microwave Theory Tech.*, **32**(4), 400–405, April 1984.

[10] R. de L. Kronig. On the theory of dispersion of X-rays. *J. Opt. Soc. Am.*, **12**(6), 547–557, 1926.

[11] G. F. Engen and C. A. Hoer. "Thru-Reflect-Line": An improved technique for calibrating the dual six-port automatic network analyzer. *IEEE Trans. Microwave Theory Tech.*, **27**, 987–993, 1979.

[12] M. Gustafsson and S. Nordebo. Cramér–Rao lower bounds for inverse scattering problems of multilayer structures. *Inverse Problems*, **22**, 1359–1380, 2006.

[13] A. D. Ioannidis, G. Kristensson, and D. Sjöberg. On the dispersion equation for a homogeneous, bi-isotropic waveguide of arbitrary cross-section. *Microwave Opt. Techn. Lett.*, **51**(11), 2701–2705, 2009.

[14] A. D. Ioannidis, G. Kristensson, and D. Sjöberg. The propagation problem in a bi-isotropic waveguide. *Progress in Electromagnetics Research B*, **19**, 21–40, 2010.

[15] J. D. Jackson. *Classical Electrodynamics*. John Wiley & Sons, New York, third edition, 1999.

[16] S. M. Kay. *Fundamentals of Statistical Signal Processing, Estimation Theory*. Prentice-Hall, Inc., NJ, 1993.

[17] M. H. A. Kramers. La diffusion de la lumière par les atomes. *Atti. Congr. Int. Fis. Como*, **2**, 545–557, 1927.

[18] A. M. Nicolson and G. F. Ross. Measurement of the intrinsic properties of materials by time-domain techniques. *IEEE Trans. Instrumentation and Measurement*, **19**, 377–382, 1970.

[19] D. M. Pozar. *Microwave Engineering*. John Wiley & Sons, New York, third edition, 2005.

[20] D. Sjöberg. Determination of propagation constants and material data from waveguide measurements. *Progress in Electromagnetics Research B*, **12**, 163–182, 2009.

[21] S. T. Smith. Statistical resolution limits and the complexified Cramér–Rao bound. *IEEE Trans. Signal Process.*, **53**(5), 1597–1609, May 2005.

[22] W. B. Weir. Automatic measurement of complex dielectric constant and permeability at microwave frequencies. *Proc. IEEE*, **62**, 33–36, 1974.